Characterization of tumor microenvironment and cell interaction patterns in testicular and diffuse large B-cell lymphomas

Matias Autio,[1-3] Oscar Brück,[4,5] Marjukka Pollari,[1,3,6] Marja-Liisa Karjalainen-Lindsberg,[7] Klaus Beiske,[8] Judit Mészaros Jørgensen,[9] Harald Holte,[10] Teijo Pellinen,[11] Suvi-Katri Leivonen[1-3] and Sirpa Leppä[1-3]

[1]Research Programs Unit, Applied Tumor Genomics, University of Helsinki, Helsinki, Finland; [2]Department of Oncology, University of Helsinki and Helsinki University Hospital Comprehensive Cancer Center, Helsinki, Finland; [3]iCAN Digital Precision Medicine Flagship, Helsinki, Finland; [4]Hematoscope Lab, Comprehensive Cancer Center & Center of Diagnostics, Helsinki University Hospital, Helsinki, Finland; [5]Department of Oncology, University of Helsinki, Helsinki, Finland; [6]Department of Oncology, Tampere University Hospital, Tampere, Finland; [7]Department of Pathology, Helsinki University Hospital, Helsinki, Finland; [8]Department of Pathology, Oslo University Hospital, Oslo, Norway; [9]Department of Hematology, Aarhus University Hospital, Aarhus, Denmark; [10]Department of Oncology, and KG Jebsen Centre for B Cell Malignancies, Oslo University Hospital, Oslo, Norway and [11]Institute for Molecular Medicine Finland (FIMM), Helsinki, Finland

Characterization of tumor microenvironment and cell interaction patterns in testicular and diffuse large B-cell lymphomas

Autio et al.

Supplementary Materials and Methods

Methods

Multiplex IHC

Antibody staining panels

	Panel 1	Panel 2	Panel 3	Panel 4
TSA-488	R-anti-Granzyme B (Abcam;ab4059) 1:500	R-anti-Lag3 (Abcam;180187, clone EPR4392(2)) 1:400	M-anti-CD4 (Thermo;MA5-12259, clone 4B12) 1:50	M-anti-Tbet (Abcam;91109, clone 4B10) 1:50
TSA-555	M-anti-OX-40 (Thermo;14-1347-82, clone ACT35) 1:50	M-anti-PD-1 (LSBio;B12784, clone 3C6) 1:100	R-anti-CD3 (Thermo; MA5-14482, clone EP449E) 1:1500	R-anti-CD3 (Thermo; MA5-14482, clone EP449E) 1:1500
Alexa-647	R-anti-Ki67 (Thermo;9106-S0, clone SP6) 1:200	R-anti-Tim3 (CST[1];45208, clone D5D5R) 1:100	R-anti-Tim3 (CST;45208, clone D5D5R) 1:100	M-anti-FoxP3 (Abcam;20034, clone 236A/E7) 1:25
Alexa-750	M-anti-CD8 (Dako; M7103, clone C8/144B) 1:200	M-anti-CD8 (Dako; M7103, clone C8/144B) 1:200	M-anti-Lag3 (LSbio;C18692, clone 17B4) 1:50	R-anti-CD4 (Abcam;ab133616, clone EPR6855) 1:25
TSA-750			R-anti-CD4 (Abcam; Ab133616, clone EPR6855) 1:1000	

[1]CST, Cell Signaling Technologies

	Panel 5	**Panel 6**	**Panel 7**
1st round			
TSA-488	M-anti-CD68 (Abcam; ab955, clone KP1) 1:200	M-anti-PD-1 (LSBio; B12784, clone 3C6) 1:200	M-anti-CD3 (Abcam; ab17143, clone F7.2.38 1:100; 1,5h RT
TSA-555	R-anti-PD-L1 (CST[1]; 13684) 1:200	R-anti-PD-L1 (CST; 13684) 1:200	R-anti-CD56 (Cell Marque; 156R-95) 1:1000
Alexa-647	R-anti-Tim-3 (CST; 45208, clone D5D5R) 1:100	R-anti-CD4 (Abcam; ab133616, clone EPR6855) 1:50	R-anti-Tim-3 (CST; 45208, clone D5D5R 1:100
Alexa-750	M-anti-CD20 (Thermo; MS-340-s, clone L26) 1:50	M-anti-CD68 (Abcam; ab955, clone KP1) 1:50	M-anti-CD45 (Dako; M0701, clone 2B11 + PD7/26) 1:50
Bleach boil			
2nd round			
Alexa 647		M-anti-CD3 (Abcam; ab17143, clone F7.2.38) 1:50	
Alexa-750	R-anti-CD163 (Abcam; ab188571, clone EPR14643) 1:200	R-anti-CD163 (Abcam; ab188571, clone EPR14643) 1:200	R-anti-Granzyme B (Abcam; ab4059) 1:100

[1]CST, Cell Signaling Technologies

We performed multiplex immunohistochemistry (mIHC) as described earlier[1-3]. We used AlexaFluor488 and AlexaFluor555 channels amplified using tyramide signal amplification (TSA) (PerkinElmer, Waltham, MA) to detect two targets. We used AlexaFluor 647 and AlexaFluor750 fluorochrome-conjugated secondary antibodies without amplification to detect two other targets using a pair of primary antibodies raised in different species. We used DAPI to counterstain nuclei and mounted and applied coverslips on the slides. In panel 3, due to weak CD4 signal, we re-stained and TSA-amplified CD4 using TSA Biotin System (#NEL700A001KT, PerkinElmer) and Streptavidin, AlexaFluor™ 750 conjugate (S21384, Thermo Fischer Scientific). In panels 5-7, after

first-round staining and whole-slide imaging of the TMAs, we soaked the slides in wash buffer at 4°C to remove the coverslips. We then bleached the previous AlexaFluor staining by soaking the slides in TBS buffer containg 25mM NaOH and 4.5%. Finally, to denature the antibodies from the first-round staining, we heated the slides in 1mM Tris/ 10mM EDTA pH9 solution for 20 minutes at 99°C. We then performed a second-round staining using AlexaFluor647 and AlexaFluor750 secondary antibodies to detect one or two additional targets.

Imaging

We used Zeiss Axio Scan.Z1 with Zeiss 20X (0.8NA, M27) Plan-Apochromat objective, Hamamatsu ORCA-Flash 4.0 V2 Digital CMOS camera (16-bit; 0.325 μm/pixel resolution), and Zeiss Colibri.7 LED Light Source to acquire digital, fluorescence images of mIHC slides. Following filter specifications were used: DAPI cube (Zeiss Filter Set 02), FITC cube (Zeiss filter Set 38 HE), Cy3 cube (Chroma technology Corp 49004 ET CY3/R), Cy5 cube (Chrome Technology Corp 49006 ET CY5), Cy7 cube (Chrome Technology Corp 49007 ET CY7). After image acquisition, we converted images to 8-bit JPEG2000 format (95% quality for panels 1-4 and 100% quality for panels 5-7).

Image analysis

We filtered out areas with staining artefacts due to autofluorescence using Ilastik (version 1.3.3). We then used CellProfiler (version 3.1.8) to perform image analysis. We used pixel co-localization to determine cell classes. We thresholded each channel intensity using Adaptive Otsu. We used "MaskImage" to determine double or triple channel positive pixels, "MeasureImageAreaOccupied" to determine thresholded channel pixel areas and counted areal proportions by dividing the area with pixel area occupied by all the channels combined (ImageMath Add command). We used "ExportToSpreadsheet" to export cell class areas as CSV files. For slides stained with panels 5-7, we also performed cell interaction analyses. First, we used CellProfiler (version 3.1.8) to perform cell segmentation on fluorescence images of the mIHC slides converted to 8-bit JPEG2000 format

(100% quality). We used Adaptive Otsu to threshold each channel intensity. We separated

clumped objects based on intensity. We determined the quality of TMA cores by visual inspection

and excluded low quality cores (e.g. ruptured or folded tissue) from further analyses.

Cell interaction analyses

As previously described, we performed cell-cell interaction analyses on the samples stained with

panels 5-7 using the method developed by Brück et al.[4]. After segmentation, we calculated the

Euclidean distance between the center points of each cell. We defined interacting cells as cells

situated closer than 100 pixels (22µm) from each other. We then calculated an interaction index I_{ab}

using the formula:

$$I_{ab} = \frac{\sum_0^{ab} i_{ab}}{\sqrt{\frac{\sum a}{\sum c} \times \frac{\sum b}{\sum c}}}$$

where i_{ab} is the interaction between any two cells a and b, $\sum a$ is the sum of cells a, $\sum b$ is the sum

of cells b, and $\sum c$ is the sum of all cells in the sample.

References

1. Autio M, Leivonen SK, Brück O, et al. Immune cell constitution in the tumor microenvironment predicts the outcome in diffuse large B-cell lymphoma. Haematologica. 2021;106(3):718-729.
2. Autio M, Leivonen SK, Brück O, Karjalainen-Lindsberg ML, Pellinen T, Leppä S. Clinical Impact of Immune Cells and Their Spatial Interactions in Diffuse Large B-Cell Lymphoma Microenvironment. Clin Cancer Res. 2022;28(4):781-792.
3. Pollari M, Pellinen T, Karjalainen-Lindsberg ML, Kellokumpu-Lehtinen PL, Leivonen SK, Leppä S. Adverse prognostic impact of regulatory T-cells in testicular diffuse large B-cell lymphoma. Eur J Haematol. 2020;105(6):712-721.
4. Brück O, Lee MH, Turkki R, et al. Spatial immunoprofiling of the intratumoral and peritumoral tissue of renal cell carcinoma patients. Mod Pathol. 2021;34(12):2229-2241.
5. Reddy A, Zhang J, Davis NS, et al. Genetic and Functional Drivers of Diffuse Large B Cell Lymphoma. Cell. 2017;171(2):481-494.e415.
6. Kotlov N, Bagaev A, Revuelta MV, et al. Clinical and Biological Subtypes of B-cell Lymphoma Revealed by Microenvironmental Signatures. Cancer Discov. 2021;11(6):1468-1489.
7. Schmitz R, Wright GW, Huang DW, et al. Genetics and Pathogenesis of Diffuse Large B-Cell Lymphoma. N Engl J Med. 2018;378(15):1396-1407.

Supplementary Tables

Table S1. Patient characteristics

Characteristics	DLBCL, NOS GE cohort n (%)*	DLBCL, NOS mIHC cohort n (%)	T-DLBCL GE cohort n (%)	T-DLBCL mIHC cohort n (%)	Reddy et al. cohort n (%)
No of patients	69 (100)	175 (100)	60 (100)	80 (100)	496 (100)
Age					
median (range)	55 (22-65)	61 (16-84)	69 (36-83)	70 (36-92)	
<60	46 (67)	83 (47)	16 (27)	17 (21)	205 (41)
≥60	23 (33)	92 (53)	44 (73)	62 (78)	268 (54)
nd				1 (1)	23 (5)
Sex					
Male	49 (71)	102 (58)	60 (100)	80 (100)	270 (54)
Female	20 (29)	73 (42)			226 (46)
Cell-of-origin					
GCB†	24 (35)	61 (35)			217 (44)
ABC	16 (23)	58 (33)			203 (41)
Unclassified	7 (10)	18 (10)			76 (15)
nd	22 (32)	38 (22)	60 (100)	80 (100)	
Subtype (Hans algorithm)					
GC	30 (43)	73 (42)	15 (25)	18 (23)	
non-GC	24 (35)	84 (48)	40 (67)	56 (70)	
nd	15 (22)	18 (10)	5 (8)	6 (8)	496 (100)
Genetic subtype					
EZB	11 (16)	17 (10)			
MCD	7 (10)	14 (8)			
BN2	1 (1)	11 (6)			
ST2	4 (6)	11 (6)			
N1	1 (1)	1 (1)			
Other	17 (25)	58 (33)			
nd	28 (41)	63 (36)	60 (100)	80 (100)	496 (100)
WHO PS					
0-1	41 (59)	123 (70)	52 (87)	61 (76)	349 (70)
≥2	28 (41)	50 (29)	8 (13)	14 (18)	112 (23)
nd		2 (1)		5 (6)	35 (7)
Stage					
I-II	8 (12)	79 (45)	39 (65)	49 (61)	179 (36)
III-IV	61 (88)	95 (54)	21 (35)	27 (34)	307 (62)
nd		1 (1)		4 (5)	10 (2)
IPI					
0-2	18 (26)	94 (54)	42 (70)	52 (65)	212 (43)
3-5	51 (74)	78 (45)	18 (30)	23 (29)	176 (35)
nd		3 (2)		5 (6)	108 (22)
Elevated LDH					
Yes	60 (87)	108 (62)	22 (37)	25 (31)	235 (47)
No	9 (13)	65 (37)	38 (63)	48 (60)	206 (42)
nd		2 (1)		7 (9)	55 (11)
EN					
0-1	25 (36)	124 (71)	47 (78)	58 (73)	341 (69)
≥2	44 (64)	45 (26)	13 (22)	17 (21)	123 (25)
nd		6 (3)		5 (6)	32 (6)
B-symptoms					
Yes	46 (67)	58 (33)	12 (20)	13 (16)	
No	23 (33)	107 (61)	48 (80)	64 (80)	
nd		10 (6)		3 (4)	
Treatment					
R-CHOP		119 (68)	32 (53)	36 (45)	
R-CHOEP‡	69 (100)	53 (30)			
other		3 (2)	28 (47)	43 (54)	
nd				1 (1)	
5-year PFS	86 %	76 %	58 %	51 %	
5-year OS	88 %	79 %	60 %	54 %	63 %

*GE, gene expression

†GCB, germinal center B-cell like; ABC, activated B-cell like; nd, not determined; IPI, international prognostic index; LDH, lactate dehydrogenase; EN, extranodal site; R-CHOP, rituximab, cyclophosphamide, doxorubicin, vincristine, prednisone; R-CHOEP, R-CHOP + etoposide

‡Patients <65 y with high-risk features were treated with R-CHOEP-14 and systemic CNS prophylaxis consisting of high-dose methotrexate and high-dose cytarabine

Table S2. Analyzed cell subtypes and their immunophenotypes.

Cell type	Immunophenotype
B cells	CD20+
T cells (TIL)	CD3+
T helper cells (Th)	CD4+CD3+
Cytotoxic T cells (Tc)	CD8+
Regulatory T cells (Treg)	Foxp3+CD4+CD3+
Macrophages (TAM)	CD68+
M1-like macrophages (M1)	CD68+CD163-
M2-like macrophages (M2)	CD163+
NK cells	CD56+CD3-CD45+

Table S3. Differentially expressed immune-related genes in ABC DLBCLs compared to GCB DLBCLs in the DLBCL, NOS gene expression cohort. Please see separate excel file.

Table S4. Differentially expressed immune-related genes in ABC DLBCLs compared to GCB DLBCLs in the Reddy et al. cohort. Please see separate excel file.

Table S5. The proportions of immune cell types in ABC DLBCLs compared to GCB DLBCLs in the DLBCL, NOS mIHC cohort. Please see separate excel file.

Table S6. Differentially expressed immune-related genes in T-DLBCLs compared to DLBCL, NOSes in the T-DLBCL and DLBCL, NOS gene expression cohorts. Please see separate excel file.

Table S7. The proportion of immune cell types in T-DLBCLs compared to DLBCL, NOSes in the mIHC cohorts. Please see separate excel file.

Supplementary Figure Legends

Figure S1. Expression of immune-related genes in germinal center B-cell like (GCB) and activated B-cell like (ABC) diffuse large B-cell lymphoma (DLBCL). A) A volcano plot depicting differently expressed immune-related genes between ABC and GCB DLBCL in the Reddy et al. cohort[5]. B) Unsupervised hierarchical clustering of patients in the Reddy et al. cohort based on the expression of the 32 most differently expressed genes between ABC and GCB DLBCL identified in the DLBCL, not otherwise specified (NOS) gene expression cohort. C-P) Boxplots depicting the expressions of *CD163* (C), *GZMB* (D), *GZMH* (E), *GZMM* (F), *PRF1* (G), *CD3D* (H), *CD3E* (I), *CD3G* (J), *CD4* (K), *CD8A* (L), *CD8B* (M), *FOXP3* (N), *TBX21* (O), and *MS4A1* (P) in GCB and ABC DLBCL in the Reddy et al. cohort. Statistical significance was analyzed using Mann-Whitney U test. LME, Lymphoma microenvironment subtypes[6].

Figure S2. Differentially expressed immune-related genes between germinal center B-cell like (GCB) and activated B-cell like (ABC) diffuse large B-cell lymphoma (DLBCL) in the Schmitz et al. cohort[7]. A) A volcano plot depicting differently expressed immune-related genes between ABC and GCB DLBCL. B) Unsupervised hierarchical clustering of patients in the Schmitz et al. cohort based on the expression of the 32 most differently expressed genes between ABC and GCB DLBCL identified in the DLBCL, not otherwise specified (NOS) gene expression cohort.

Figure S3. Proportions of immune cell subtypes in germinal center B-cell like (GCB) and activated B-cell like (ABC) diffuse large B-cell lymphoma (DLBCL) analyzed by multiplex immunohistochemistry (mIHC). A-J) Boxplots depicting the proportions of T cells/total cells (A), T helper cells/total cells (B), cytotoxic T cells/total cells (C), GrB$^+$ cells/total cells (D), PD-L1$^+$ cells/total cells (E), TIM3$^+$ M2-like macrophages/total cells (F), TIM3$^+$ T cells/total cells (G), PD-1$^+$ T cells/total cells (H), PD-1$^+$ T helper cells/total cells (I), and CD20$^-$ cells/total cells (J) in GCB and

ABC DLBCL analyzed by mIHC in the DLBCL, not otherwise specified (NOS) mIHC cohort. Statistical significance was analyzed using Mann-Whitney U test. Due to staining errors, data on certain cell types was unavailable for some samples. K) A barplot depicting the proportion of GCB and ABC DLBCL samples staining positive for HLA-ABC, B2M, and HLA-DR analyzed by IHC in the DLBCL, NOS mIHC cohort. Statistical significance was analyzed using Mann-Whitney U test. Due to staining errors, data on certain cell types was unavailable for some samples. T cells=CD3$^+$ cells, Th cells=CD4$^+$CD3$^+$ cells, Tc cells=CD8$^+$ cells, M2-like=CD163$^+$ cells.

Figure S4. Proportions of immune cells in HLA and B2M positive and negative diffuse large B-cell lymphomas (DLBCLs). A-C) Boxplots depicting the proportions of immune cell subtypes in HLA-ABC (A), B2M (B), and HLA-DR (C) negative and positive DLBCL samples analyzed by multiplex immunohistochemistry (mIHC) in the DLBCL, not otherwise specified (NOS) mIHC cohort. Statistical significance was analyzed using Mann-Whitney U test. Due to staining errors, data on certain cell types was unavailable for some samples. T cells=CD3$^+$ cells, Th cells=CD4$^+$CD3$^+$ cells, Tc cells=CD8$^+$ cells, Tregs=FOXP3$^+$CD3$^+$ cells, TAMs=CD68$^+$ cells, M2-like=CD163$^+$ cells, M1-like=CD163$^-$CD68$^+$ cells, NK cells=CD56$^+$CD3$^-$CD45$^+$ cells.

Figure S5. Differently expressed immune-related genes between testicular diffuse large B-cell lymphoma (T-DLBCL) and DLBCL, not otherwise specified (NOS). A) Unsupervised hierarchical clustering of patients in the T-DLBCL and DLBCL, NOS gene expression cohorts based on the expression of all available immune-related genes. B) A volcano plot depicting differently expressed immune-related genes between T-DLBCL and DLBCL, NOS samples in the T-DLBCL and DLBCL, NOS gene expression cohorts analyzed by Nanostring nCounter Human PanCancer Immunoprofiling Panel. C) A volcano plot depicting immune cell types whose proportions in the TME differ most between T-DLBCL and DLBCL, NOS samples in the T-DLBCL and DLBCL, NOS mIHC cohorts. Cell proportions indicate proportions of total cells except where

stated otherwise. T cells=CD3$^+$ cells, Th=CD4$^+$CD3$^+$ cells, Tc=CD8$^+$ cells,

Tregs=FOXP3$^+$CD4$^+$CD3$^+$ cells, Tregs/T cells=FOXP3$^+$CD3$^+$/CD3$^+$ cells, B cells=CD20$^+$ cells.

Figure S6. Differences in the constitution of the tumor microenvironment (TME) analyzed by multiplex immunohistochemistry (mIHC) between testicular diffuse large B-cell lymphoma (T-DLBCL) and DLBCL, not otherwise specified (NOS). A-L) Boxplots depicting the proportions of B cells/total cells (A), T cells/total cells (B), T helper cells/total cells (C), cytotoxic T cells/total cells (D), regulatory T cells/total cells (E), GrB$^+$ cells/total cells (F), macrophages/total cells (G), M1-like macrophages/total cells (H), M2-like macrophages/total cells (I), PD-1$^+$ cells/total cells (J), PD-1$^+$ T cells/total cells (K), and LAG3$^+$ T cells/total cells (L) in T-DLBCL and DLBCL, NOS samples in the T-DLBCL and DLBCL, NOS mIHC cohorts. Statistical significance was analyzed using Mann-Whitney U test. Due to staining errors, data on certain cell types was unavailable for some samples. M-U) Boxplots depicting the proportions of B cells/total cells (M), T cells/total cells (N), T helper cells/total cells (O), cytotoxic T cells/total cells (P), regulatory T cells/total cells (Q), GrB$^+$ cells/total cells (O), macrophages/total cells (R), PD-1$^+$ cells/total cells (S), PD-1$^+$ T cells/total cells (T), and LAG3$^+$ T cells/total cells (U) in germinal center (GC) and non-GC T-DLBCL as well as GCB and ABC DLBCL samples in the T-DLBCL and DLBCL, NOS mIHC cohorts. The numbers comparing different subtypes are adj. *p*-values for the Mann-Whitney U test comparing the respective groups. Due to staining errors, data on certain cell types was unavailable for some samples. V) A barplot depicting the proportion of T-DLBCL and GCB and ABC type DLBCL, NOS samples staining positive for HLA-ABC, B2M, and HLA-DR analyzed by IHC in the T-DLBCL and DLBCL, NOS mIHC cohorts. B cells=CD20$^+$ cells, T cells=CD3$^+$ cells, Th cells=CD4$^+$CD3$^+$ cells, Tc cells=CD8$^+$ cells, Tregs=FOXP3$^+$CD3$^+$ cells, TAMs=CD68$^+$ cells, M1-like=CD163$^−$CD68$^+$ cells.

Figure S7. Interactions between different immune cell subtypes in germinal center B-cell like (GCB) and activated B-cell like (ABC) diffuse large B-cell lymphoma (DLBCL) and

testicular (T)-DLBCL. A) Ballon plot depicting differences in the number of interactions between different immune cell subtypes in ABC compared to GCB DLBCL in the DLBCL, not otherwise specified (NOS) multiplex immunohistochemistry (mIHC) cohort. On the x-axis are depicted the studied cell phenotypes and, on the y-axis, their neighboring cell phenotypes. The color of the balloons shows the difference in the interaction index in ABC compared to GCB DLBCL, calculated as the 2-fold logarithm of the fold-change (FC). B) Boxplots depicting differences in the number of selected interactions between different immune cell subtypes in GCB and ABC DLBCL in the DLBCL, NOS mIHC cohort. C) Ballon plot depicting differences in the number of interactions between different immune cell subtypes in T-DLBCL compared to DLBCL, NOS samples in the DLBCL, NOS and T-DLBCL mIHC cohorts. On the x-axis are depicted the studied cell phenotypes and, on the y-axis, their neighboring cell phenotypes. The color of the balloons shows the difference in the interaction index in T-DLBCL samples compared to DLBCL, NOS samples, calculated as the 2-fold logarithm of the fold-change (FC). D) Boxplots depicting differences in the number of selected interactions between different immune cell subtypes in DLBCL, NOS and T-DLBCL samples in the DLBCL, NOS and T-DLBCL mIHC cohorts. TAM=CD68$^+$ cells, M1=CD163$^-$ CD68$^+$ cells, M2=CD163$^+$ cells, T cell=CD3$^+$ cells, B cell=CD20$^+$ cells, PD1=PD-1$^+$ cells, PDL1=PD-L1$^+$ cells, TIM3=TIM3$^+$ cells. * = adj. $p < 0.05$, ** = adj. $p < 0.01$, *** = adj. $p < 0.001$, ns = not significant.

Figure S8. Clinical impact of different immune cells and their interactions in germinal center B-cell like (GCB) and activated B-cell like (ABC) diffuse large B-cell lymphoma (DLBCL) and testicular (T)-DLBCL. A) A forest plot visualizing the impact of selected immune cell subtypes on overall survival (OS) in GCB and ABC DLBCL in the DLBCL, not otherwise specified (NOS) multiplex immunohistochemistry (mIHC) cohort, as evaluated by Cox univariable regression analyses with continuous variables. Due to staining errors, data on certain cell types was unavailable for some samples. B-G) Forest plots visualizing the impact of PD-L1$^+$TIM3$^+$ M1-like macrophages (B), macrophages (C), M2-like macrophages (D), PD-L1$^+$ cells (E), Granzyme B$^+$

cells (F), and TIM3+ T cells (G) on progression-free survival (PFS) and OS in Cox multivariable

regression analyses with International Prognostic Index (IPI) in patients with GCB DLBCL in the

DLBCL, NOS mIHC cohort. H-I) Kaplan-Meier (log-rank test) survival plots depict OS in GCB (H)

and ABC DLBCL (I) patients with high and low proportions of macrophages using median cutoff in

the DLBCL, NOS mIHC cohort. J-K) Forest plots visualizing the impact of PD-L1$^+$TIM3$^+$ M1-like

macrophages (J) and cytotoxic T cells (K) on PFS and OS in Cox multivariable regression

analyses with IPI in patients with ABC DLBCL in the DLBCL, NOS mIHC cohort. TAMs=CD68$^+$

cells, M1-like= CD163$^-$CD68$^+$ cells, M2-like=CD163$^+$ cells, T cells=CD3$^+$ cells, Tc=CD8$^+$ cells.

**Figure S9. Clinical impact of different immune cell interactions in germinal center B-cell like
(GCB) and activated B-cell like (ABC) diffuse large B-cell lymphoma (DLBCL) and testicular
(T)-DLBCL.** A) A forest visualizing the impact of selected immune cell interactions on overall

survival (OS) in GCB and ABC DLBCL in the DLBCL, not otherwise specified (NOS) multiplex

immunohistochemistry (mIHC) cohort, and in T-DLBCL in the T-DLBCL mIHC cohort, respectively,

as evaluated by Cox univariable regression analyses with continuous variables. B-D) Forest plots

visualizing the impact of M2-like macrophage-T cell interactions (B), M2-like macrophage-T helper

cell interactions (C), and M2-like macrophage-PD1 interactions (D) on progression-free survival

(PFS) and OS in Cox multivariable regression analyses with International Prognostic Index (IPI) in

patients with GCB DLBCL in the DLBCL, NOS mIHC cohort. E-J) Forest plots visualizing the

impact of M2-like macrophage-T cell interactions (E), M2-like macrophage-T helper cell

interactions (F), M2-like macrophage-PD1 interactions (G), T cell-macrophage interactions (H), T

helper cell-macrophage interactions (I), and T helper cell-T cell interactions (J) on PFS and OS in

Cox multivariable regression analyses with IPI, molecular subtype, and treatment (rituximab

containing immunochemotherapy vs. chemotherapy) in patients with T-DLBCL in the T-DLBCL

mIHC cohort. K) Kaplan-Meier (log-rank test) survival plot depicts OS in T-DLBCL patients with

high and low amounts of T-helper cell-macrophage interactions in their tumor microenvironment

(TME) using median cutoff in the T-DLBCL mIHC cohort. L-M) Kaplan-Meier (log-rank test) survival

plots depict OS (L) and PFS (M) in T-DLBCL patients treated with R-CHOP-like immunochemotherapy with high and low amounts of T-helper cell-macrophage interactions in their TME using median cutoff in the T-DLBCL mIHC cohort. TAM=CD68$^+$ cells, M2=CD163$^+$ cells, T cell=CD3$^+$ cells, Th=CD4$^+$CD3$^+$ cells, PD1=PD-1$^+$ cells.

Figure S1. Expression of immune-related genes in germinal center B-cell like (GCB) and activated B-cell like (ABC) diffuse large B-cell lymphoma (DLBCL).
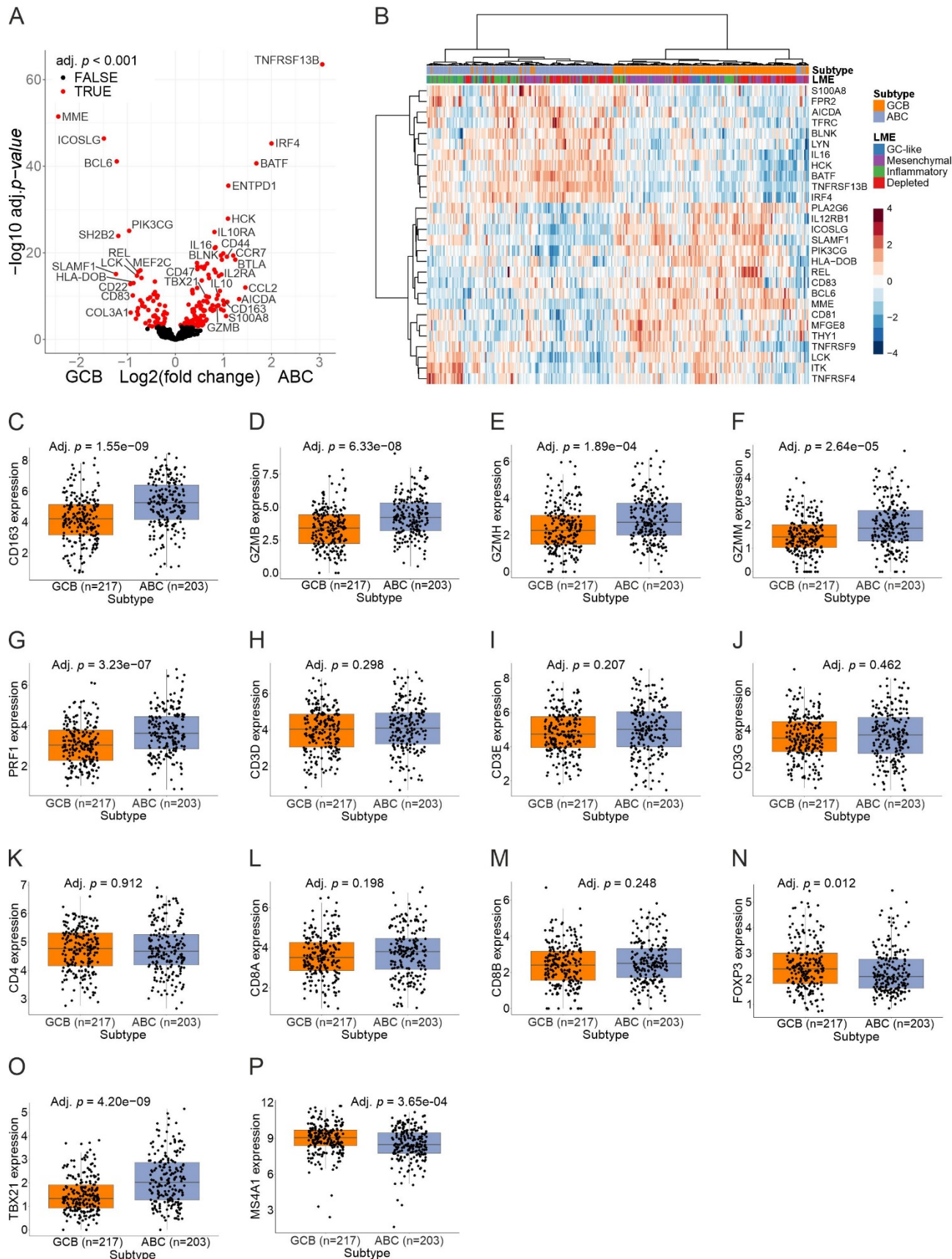
Figure S2. Differentially expressed immune-related genes between germinal center B-cell like (GCB) and activated B-cell like (ABC) diffuse large B-cell lymphoma (DLBCL) in the Schmitz et al. cohort[7].
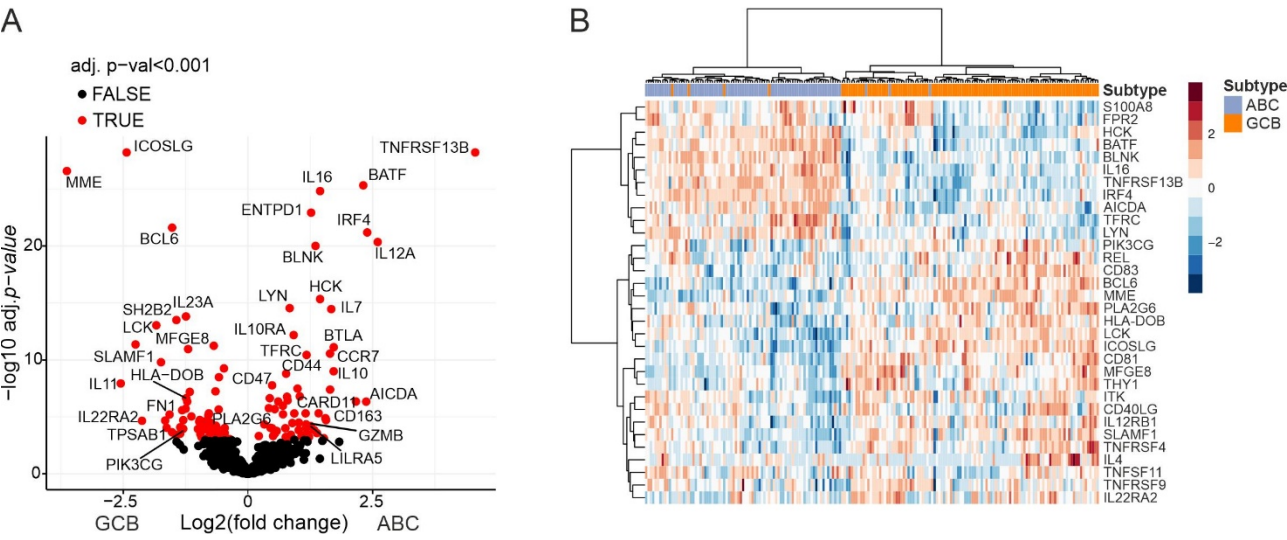
Figure S3. Proportions of immune cell subtypes in germinal center B-cell like (GCB) and activated B-cell like (ABC) diffuse large B-cell lymphoma (DLBCL) analyzed by multiplex immunohistochemistry (mIHC).
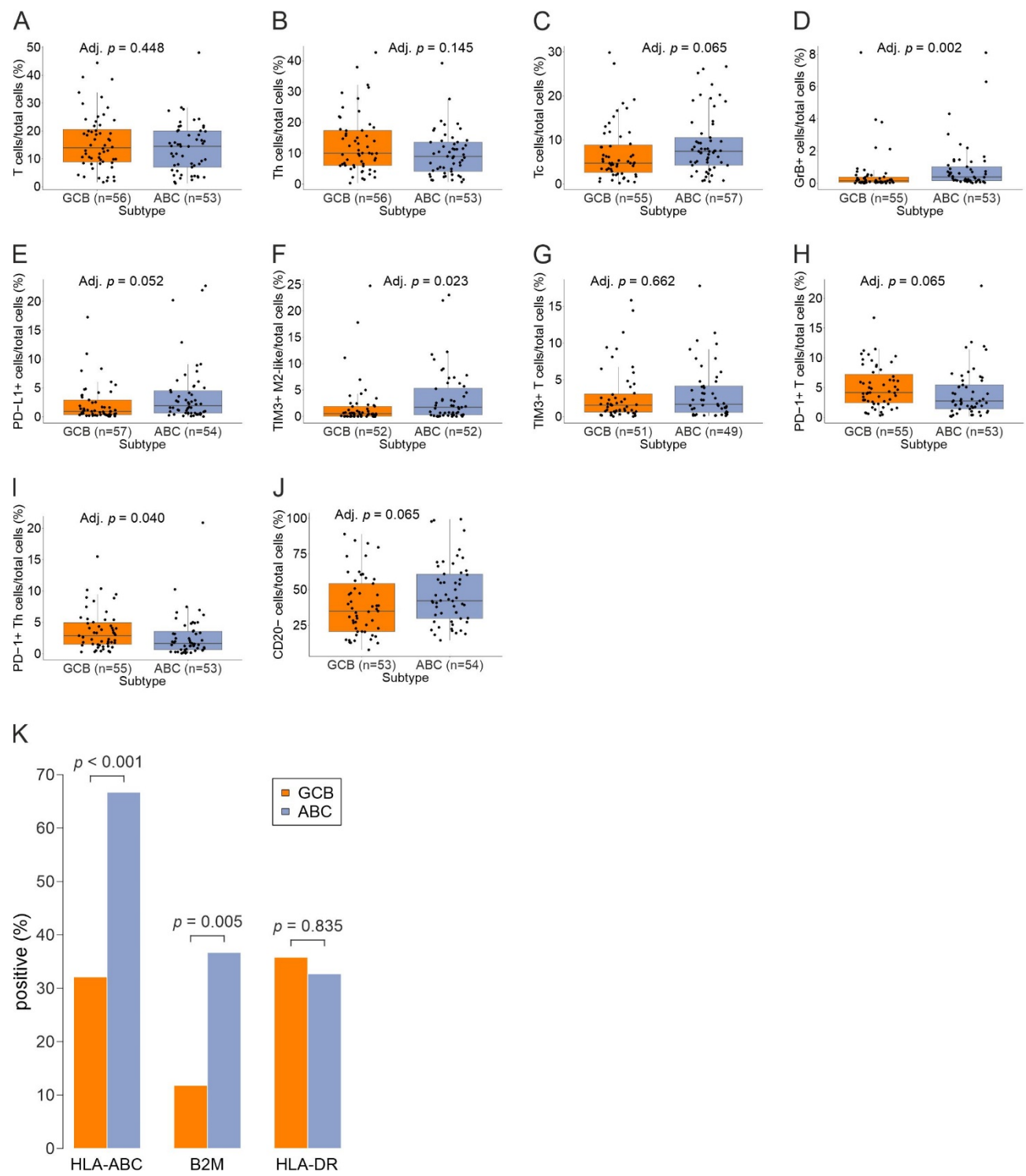
Figure S4. Proportions of immune cells in HLA and B2M positive and negative diffuse large B-cell lymphomas (DLBCLs).
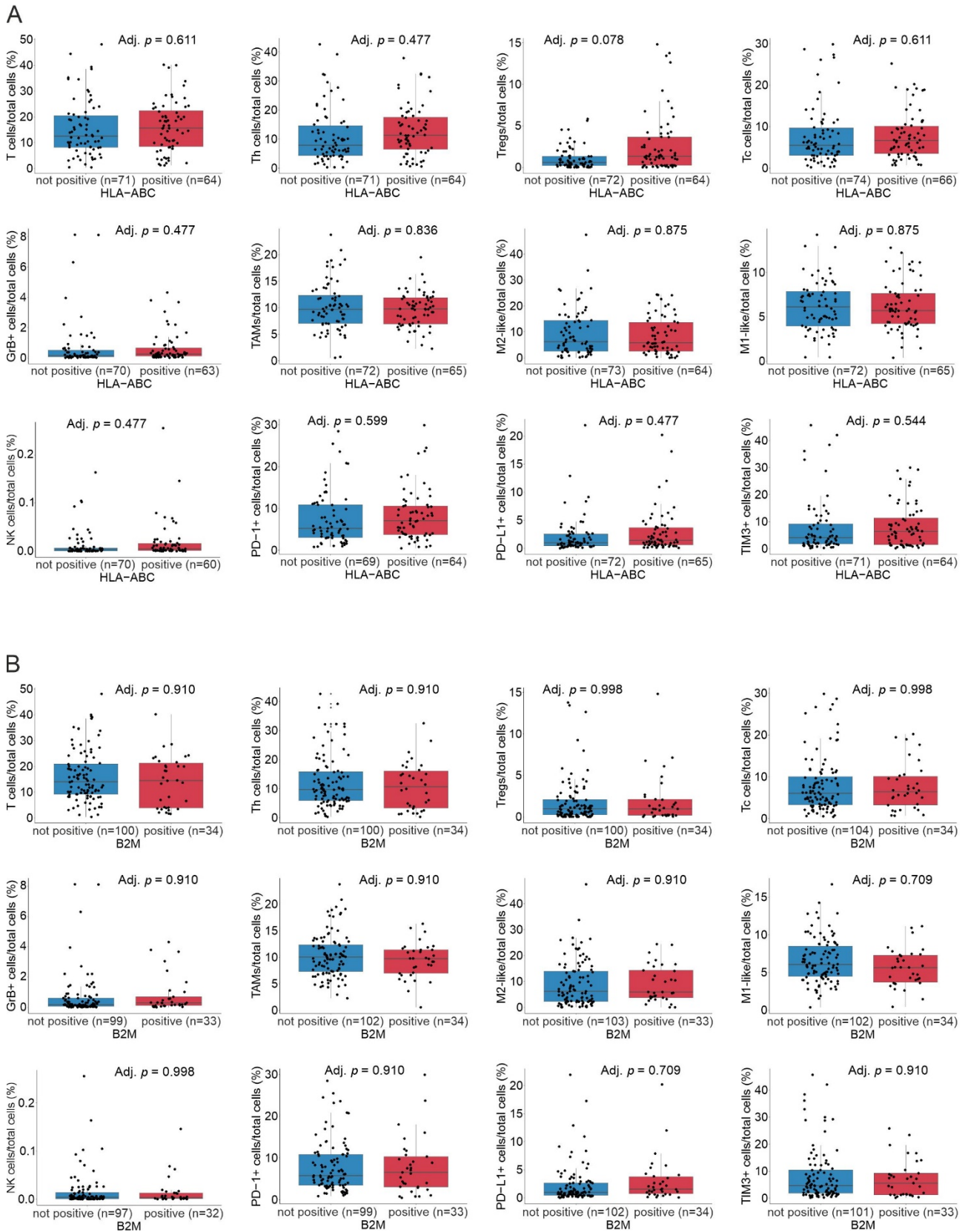
C
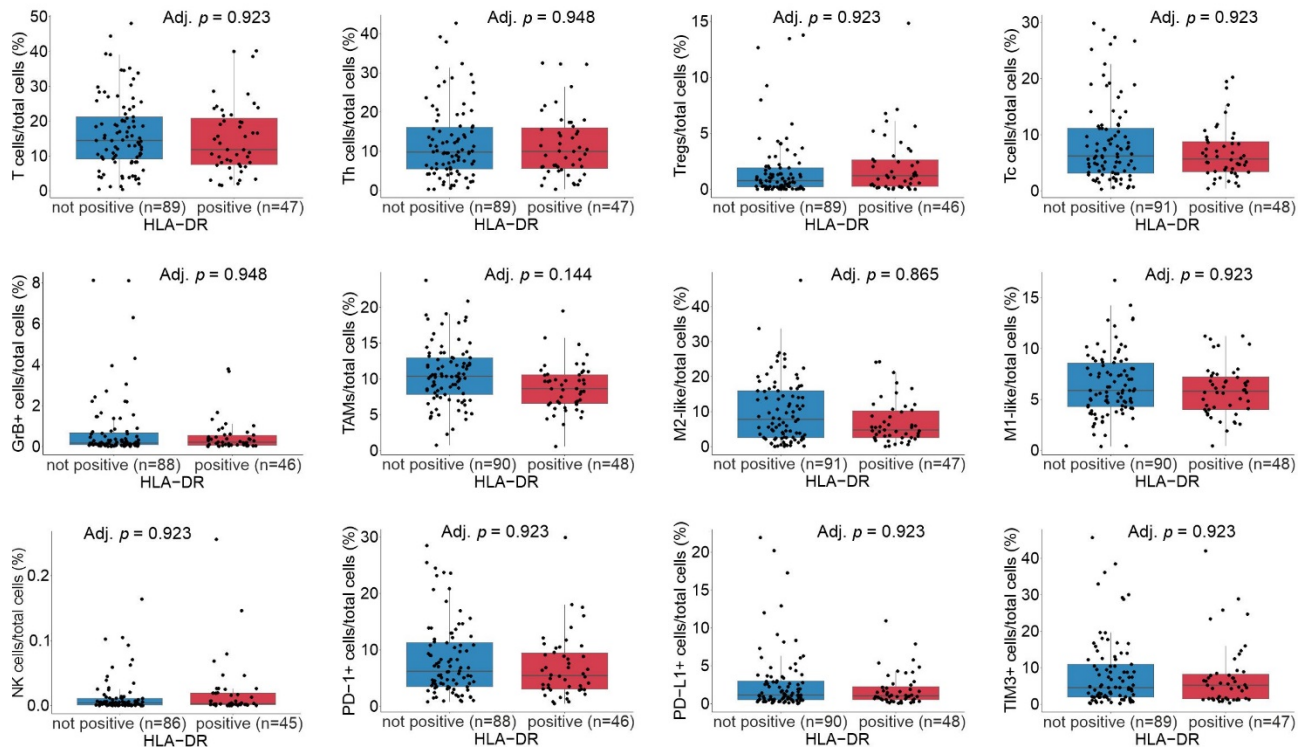
Figure S5. Differently expressed immune-related genes between testicular diffuse large B-cell lymphoma (T-DLBCL) and DLBCL, not otherwise specified (NOS).
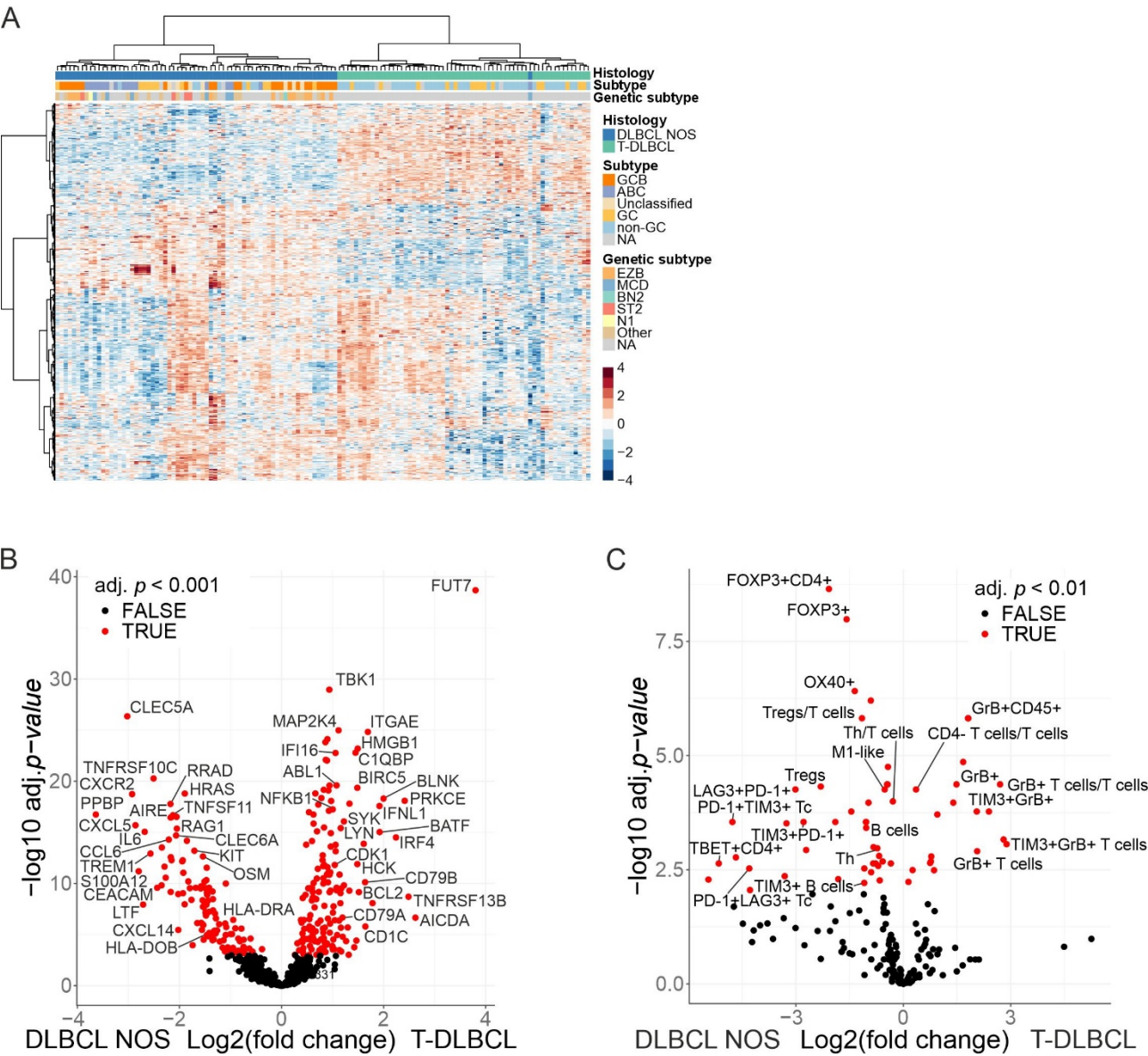
Figure S6. Differences in the constitution of the tumor microenvironment (TME) analyzed by multiplex immunohistochemistry (mIHC) between testicular diffuse large B-cell lymphoma (T-DLBCL) and DLBCL, not otherwise specified (NOS).

V

Figure S7. Interactions between different immune cell subtypes in germinal center B-cell like (GCB) and activated B-cell like (ABC) diffuse large B-cell lymphoma (DLBCL) and testicular (T)-DLBCL.

C

D

Figure S8. Clinical impact of different immune cells and their interactions in germinal center B-cell like (GCB) and activated B-cell like (ABC) diffuse large B-cell lymphoma (DLBCL) and testicular (T)-DLBCL.
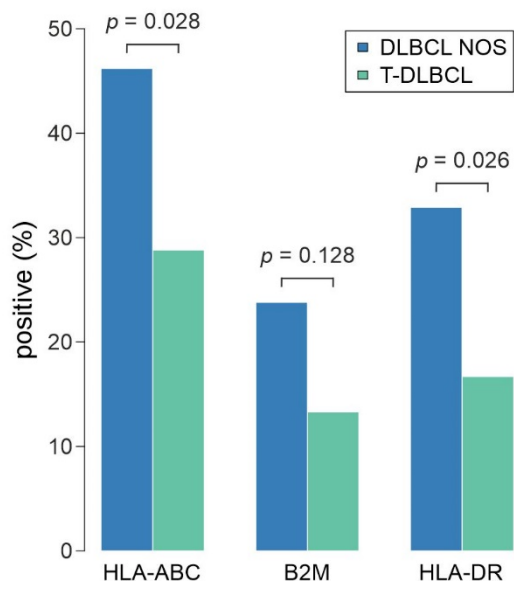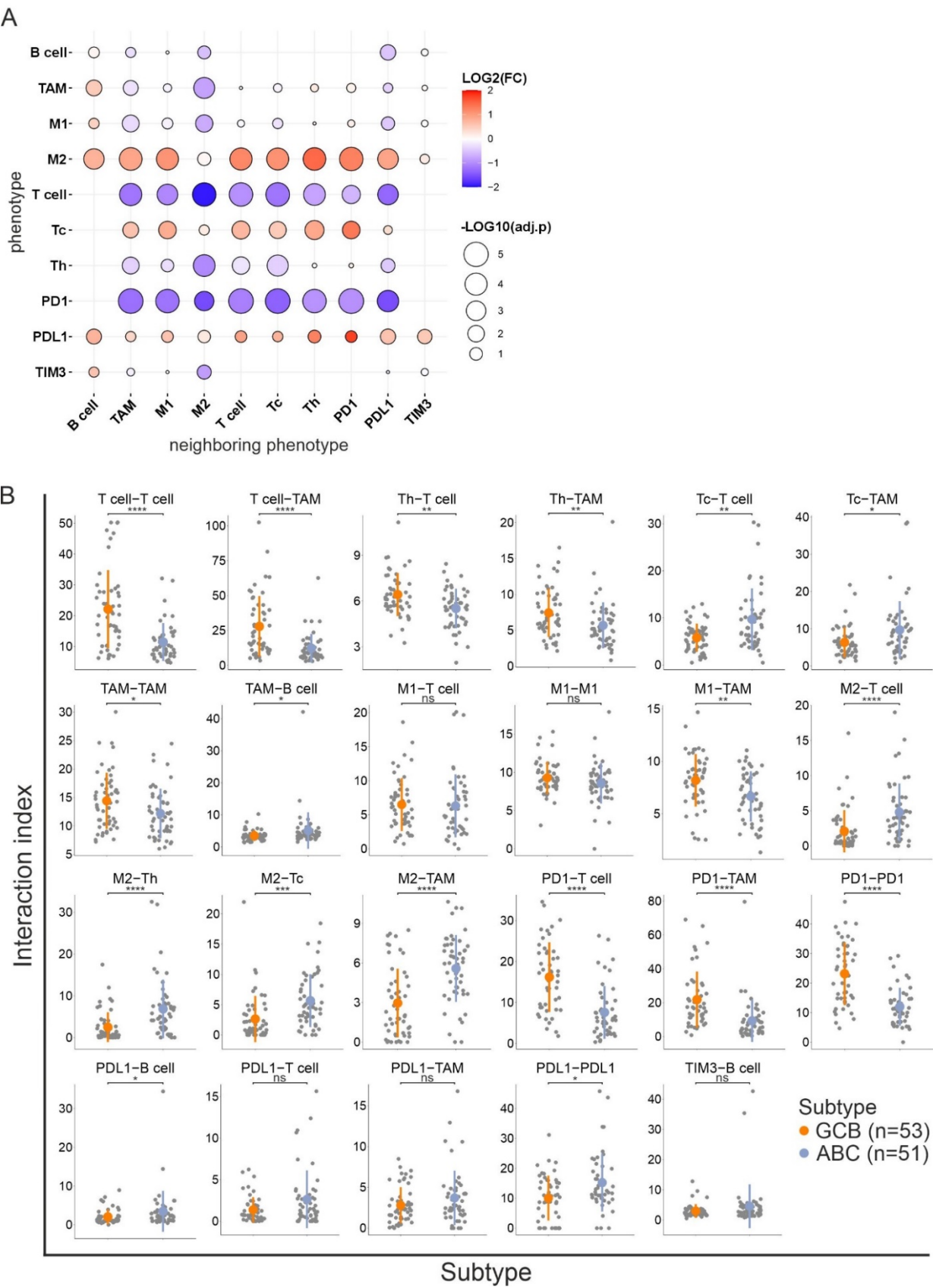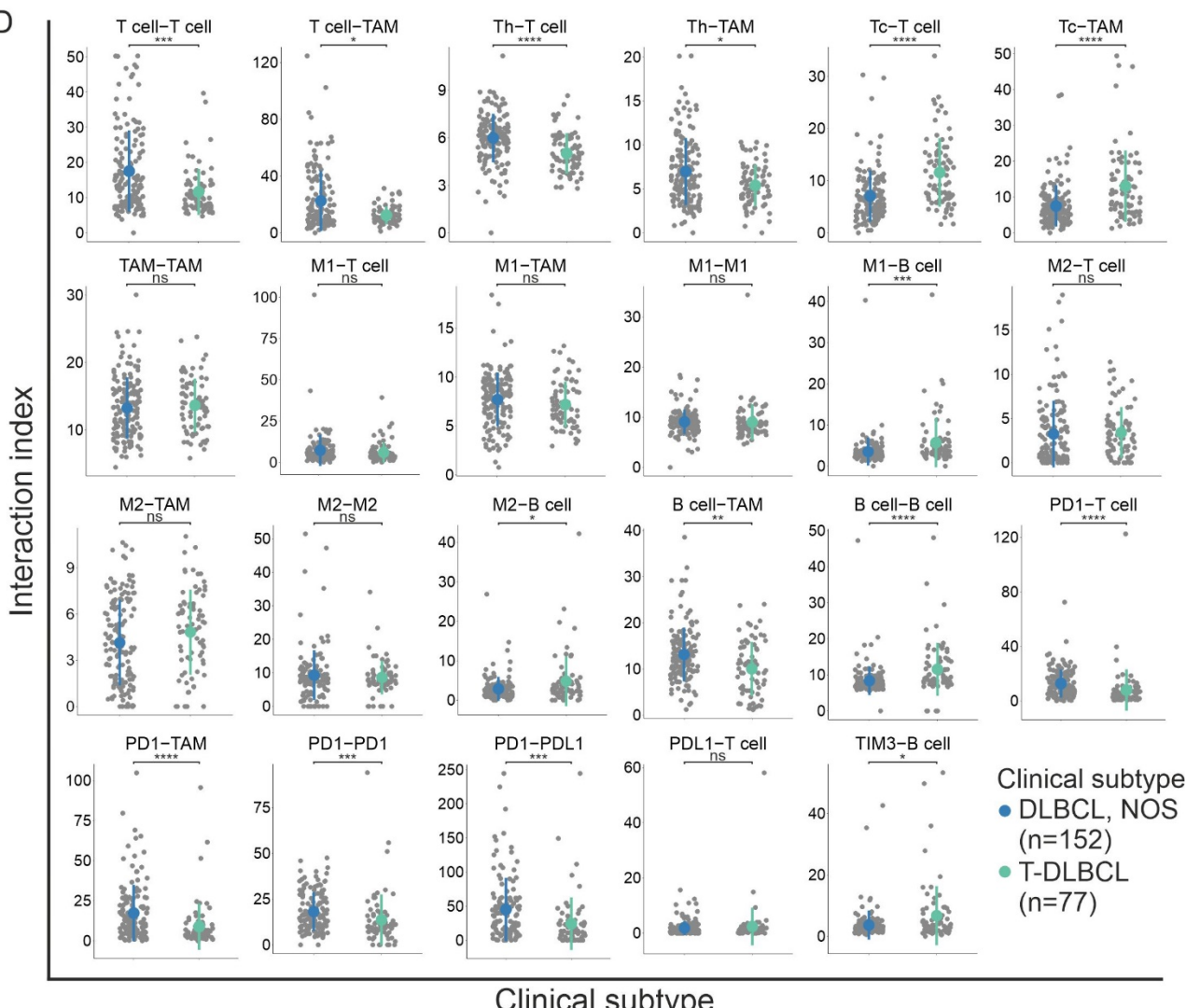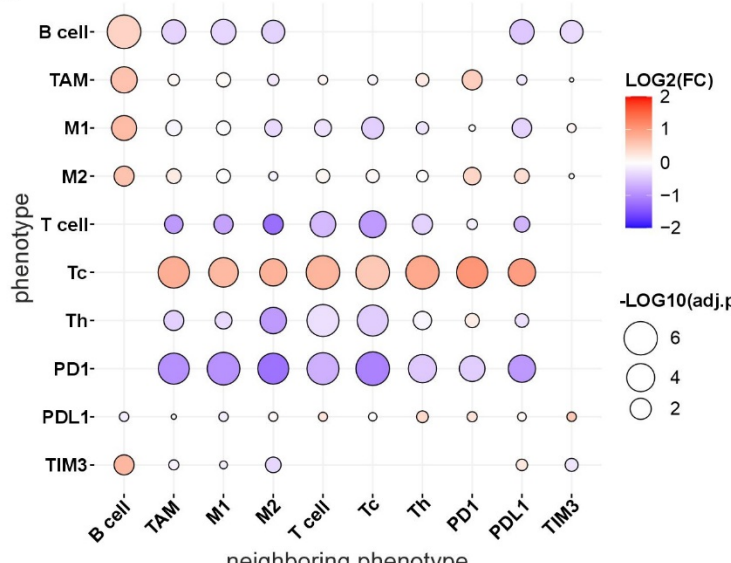
A

GCB	OS HR (95% CI)		p
PD−L1+TIM3+ M1-like (n=49)	4.73 (1.55−14.5)		0.006
TAMs (n=57)	1.34 (1.07−1.70)		0.013
M2-like (n=57)	1.07 (1.01−1.14)		0.032
PD−L1+ (n=57)	1.25 (1.07−1.45)		0.005
Granzyme B+ (n=55)	1.80 (1.16−2.79)		0.009
TIM3+ T cells (n=51)	1.28 (1.07−1.52)		0.006
Tc (n=55)	1.05 (0.92−1.20)		0.467
ABC			
PD−L1+TIM3+ M1-like (n=52)	2.68 (0.95−7.57)		0.062
TAMs (n=54)	1.07 (0.97−1.18)		0.188
M2-like (n=54)	1.00 (0.95−1.05)		0.915
PD−L1+ (n=54)	0.99 (0.92−1.08)		0.867
Granzyme B+ (n=53)	1.25 (0.98−1.60)		0.073
TIM3+ T cells (n=49)	1.04 (0.92−1.18)		0.550
Tc (n=57)	0.92 (0.84−1.00)		0.053

0.5 1.0 2.0 5.0

B

GCB	PFS HR (95% CI)		p
PD−L1+TIM3+ M1-like	2.85 (1.01−8.00)		0.047
IPI 3−5	1.01 (0.21−4.87)		0.993

0.5 1.0 2.0 5.0 10.0

GCB	OS HR (95% CI)		p
PD−L1+TIM3+ M1-like	4.25 (1.28−14.1)		0.018
IPI 3−5	1.72 (0.26−11.4)		0.574

0.5 1.0 2.0 5.0 10.0

C

GCB	OS HR (95% CI)		p
TAMs	1.33 (1.04−1.69)		0.021
IPI 3−5	1.87 (0.30−11.5)		0.500

0.5 1.0 2.0 5.0

D

GCB	PFS HR (95% CI)		p
M2-like	1.06 (0.99−1.13)		0.076
IPI 3−5	1.00 (0.19−5.23)		0.996

0.5 1.0 2.0 5.0

GCB	OS HR (95% CI)		p
M2-like	1.06 (0.99−1.13)		0.088
IPI 3−5	2.14 (0.31−14.7)		0.441

0.5 1.0 2.0 5.0

E

GCB	PFS HR (95% CI)		p
PD−L1+	1.16 (1.00−1.35)		0.043
IPI 3−5	1.22 (0.27−5.47)		0.796

0.5 1.0 2.0 5.0

GCB	OS HR (95% CI)		p
PD−L1+	1.26 (1.06−1.49)		0.008
IPI 3−5	2.60 (0.42−16.1)		0.305

0.5 1.0 2.0 5.0

F

GCB	PFS HR (95% CI)		p
Granzyme B+	1.50 (1.03−2.18)		0.034
IPI 3−5	1.05 (0.21−5.36)		0.949

0.5 1.0 2.0 5.0

GCB	OS HR (95% CI)		p
Granzyme B+	1.70 (1.07−2.68)		0.024
IPI 3−5	2.08 (0.30−14.3)		0.455

0.5 1.0 2.0 5.0

G

GCB	PFS HR (95% CI)		p
TIM3+ T cells	1.22 (1.04−1.44)		0.018
IPI 3−5	1.18 (0.21−6.53)		0.849

0.5 1.0 2.0 5.0

GCB	OS HR (95% CI)		p
TIM3+ T cells	1.25 (1.05−1.50)		0.014
IPI 3−5	1.82 (0.27−12.2)		0.540

0.5 1.0 2.0 5.0

H GCB DLBCL

TAMs — Low — High

Survival probability / OS (mo)
p = 0.016

Number at risk

	0	20	40	60	80	100	120
Low	28	28	26	18	5	2	1
High	29	27	26	13	1	0	0

I ABC DLBCL

TAMs — Low — High

Survival probability / OS (mo)
p = 0.860

Number at risk

	0	20	40	60	80	100	120
Low	27	23	18	7	3	3	0
High	27	22	17	10	3	0	0

J

ABC	PFS HR (95% CI)		p
PD−L1+TIM3+ M1-like	2.07 (0.69−6.20)		0.193
IPI 3−5	2.24 (0.78−6.49)		0.136

0.5 1.0 2.0 5.0 10.0

ABC	OS HR (95% CI)		p
PD−L1+TIM3+ M1-like	1.94 (0.64−5.90)		0.245
IPI 3−5	2.10 (0.72−6.10)		0.174

0.5 1.0 2.0 5.0 10.0

K

ABC	PFS HR (95% CI)		p
Tc	0.91 (0.83−1.00)		0.058
IPI 3−5	2.55 (0.94−6.93)		0.067

0.5 1.0 2.0 5.0

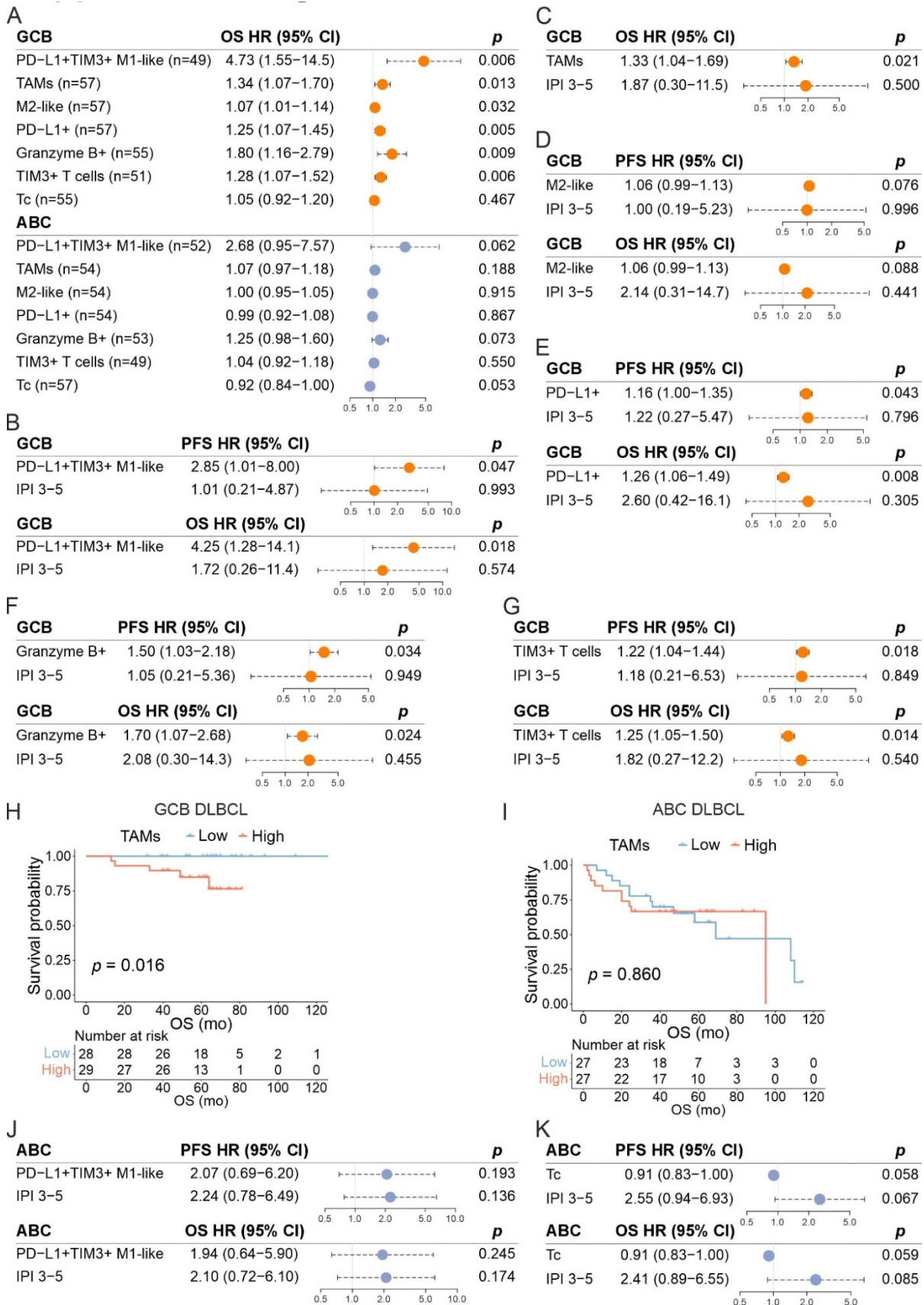| ABC	OS HR (95% CI)		p
Tc	0.91 (0.83−1.00)		0.059
IPI 3−5	2.41 (0.89−6.55)		0.085

0.5 1.0 2.0 5.0

Figure S9. Clinical impact of different immune cell interactions in germinal center B-cell like (GCB) and activated B-cell like (ABC) diffuse large B-cell lymphoma (DLBCL) and testicular (T)-DLBCL.

J

T-DLBCL	PFS HR (95% CI)		*p*
Th−T cell	0.71 (0.53−0.95)		0.023
IPI 3−5	6.40 (2.81−14.6)		<0.001
non−GC	3.88 (1.55−9.71)		0.004
immunochemotherapy	0.23 (0.11−0.51)		<0.001

0.1 0.5 1.0 2.0 5.0 15.0

T-DLBCL	OS HR (95% CI)		*p*
Th−T cell	0.76 (0.55−1.06)		0.105
IPI 3−5	7.09 (2.95−17.0)		<0.001
non−GC	2.59 (1.03−6.54)		0.044
immunochemotherapy	0.29 (0.12−0.66)		0.003

0.1 0.5 1.0 2.0 5.0 15.0

K T-DLBCL

L T-DLBCL

M T-DLBCL

26